



Characterization and separation of cancer cells with a wicking fiber device

Suzanne M. Tabbaa^{1,2}, Julia L. Sharp³, and Karen J.L. Burg^{1,2,4}

¹Department of Bioengineering; Clemson University, Clemson, SC 29634, United States

²Institute for Biological Interfaces of Engineering; Clemson University, Clemson, SC 29634, United States

³Department of Mathematical Sciences; Clemson University, Clemson, SC 29634, United States

⁴Department of Small Animal Medicine & Surgery; University of Georgia, Athens, GA 30602, United States

Abstract

Current cancer diagnostic methods lack the ability to quickly, simply, efficiently, and inexpensively screen cancer cells from a mixed population of cancer and normal cells. Methods based on biomarkers are unreliable due to complexity of cancer cells, plasticity of markers, and lack of common tumorigenic markers. Diagnostics are time intensive, require multiple tests, and provide limited information. In this study, we developed a novel wicking fiber device that separates cancer and normal cell types. To the best of our knowledge, no previous work has used vertical wicking of cells through fibers to identify and isolate cancer cells. The device separated mouse mammary tumor cells from a cellular mixture containing normal mouse mammary cells. Further investigation showed the device separated and isolated human cancer cells from a heterogeneous mixture of normal and cancerous human cells. We report a simple, inexpensive, and rapid technique that has potential to identify and isolate cancer cells from large volumes of liquid samples that can be translated to on-site clinic diagnosis.

Key Terms

Biomarkers, cancer, cell movement, circulating tumor cell, *in vitro* diagnostic

Introduction

Current methods to diagnose and analyze the presence and progression of cancer involve histological and genetic analysis of a solid tumor to predict the stage of the cancer¹. A major limitation of this type of diagnosis is the heterogeneity of the tumor as well as the fact that the analysis occurs after a palpable tumor has formed. Tumors are reported to have different subpopulations of cancer cells with varying phenotypes and degrees of tumor-initiating capabilities². The subpopulations of cancer cells create tumorigenic regions and non-tumorigenic regions within the tumor³. This regionality limits the ability for a single biopsy to capture complete information about the tumor¹. Common biopsy analysis involves detecting phenotypic and genotypic biomarkers; this type of analysis is unreliable and lacks specificity due to the heterogeneous phenotype and genotype of cancer cells^{3,4,5,6}. The standard techniques to

analyze a tumor biopsy are time-consuming, expensive, provide limited information regarding the metastatic potential of subpopulations within the tumor, and require multiple forms of off-site analysis to confirm results. Most importantly, tumor interrogation occurs only after a mass has been identified, i.e. after the cancer process has evolved.

Other diagnostic techniques are shifting from invasive tissue analysis toward liquid biopsy analysis, e.g. blood biopsy, which has the potential to detect the initial occurrence of cancer. A minimally invasive blood biopsy sample can be used for detecting circulating tumor cells (CTCs) and diagnosing the cancer stage, monitoring treatments, and providing insight into the metastatic process⁷. However, major limitations for detecting CTCs are the exceedingly low concentrations of CTCs in blood samples and the heterogeneous phenotypes within the CTC population^{8,9}. As a result, the current CTC detection and isolation



systems have low capture efficiencies and low specificities. Technologies for CTC detection and separation include macro-scale systems and microfluidics that use physical characteristics of the cells as well as cell surface labels. Most macro-scale systems use antibody-dependent techniques that detect epithelial markers to target CTCs. These approaches assume all CTCs are expressing epithelial markers, which limits these approaches to a specific subpopulation of CTCs. Aggressive CTC populations commonly exhibit mesenchymal phenotypes in the bloodstream and, because they lack the epithelial markers that current CTC technologies target, go undetected^{10,11,12,13,14}. Other CTC detection methods include microfluidic devices and chips that use both antigen-dependent and antigen-independent techniques to detect and separate cancer cells. These approaches have better specificity and isolation efficiency but are restricted to small volumes of sample and low yield of isolated CTCs^{8,15}.

We have developed a wicking fiber device that may lead to a simple and low cost approach to rapidly identify and capture cancer cells. A wicking fiber (**Fig. 1**) has a non-circular, grooved cross-section with channels that run the length of the fiber. The unique configuration facilitates and enhances wicking by capillary action along the channels. These fibers were originally used to improve wicking properties of textiles, but were later used at the stationary phase in chromatography applications such as proteomic separation and metal extraction processes^{16,17,18}. Our research group established the use of wicking fibers to tissue engineering applications to improve vascularity and cell growth in scaffolds¹⁹. The aim of the current study was to evaluate the capability of wicking fibers to isolate cancer cells from a heterogeneous cellular liquid. We demonstrated the wicking fiber device separates (1) a mixture of normal mouse mammary epithelial cells (MMTV-neu) from mouse epithelial breast cancer cells (NMuMG) and (2) malignant human breast epithelial cells (MCF-7) and benign human breast epithelial cells (MCF-10A).

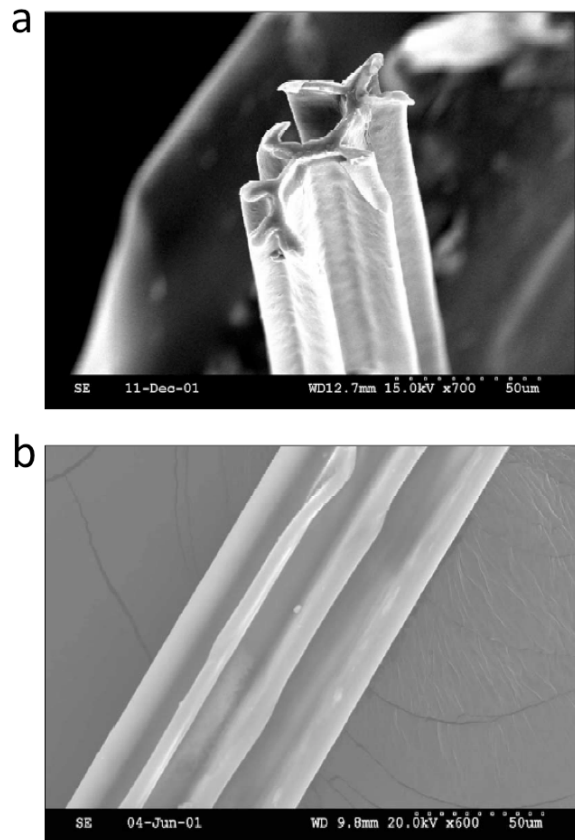


Figure 1. Scanning electron microscope (SEM) image of a wicking fiber. Reprinted from Journal of Chromatography A, Vol. 986, R.K. Marcus et al., Capillary-channeled polymer fibers as stationary phases in liquid chromatography separations, pp. 17-31. 2003, with permission from Elsevier²⁰. (a) Image of non-circular grooved cross-section and parallel channels of the wicking fiber which facilitate strong wicking action and greatly increase surface area^{20,21}. (b) Image depicts the long axis of the wicking fiber, with parallel channels along the length of the fiber.

Methods and Materials

Cell culture of mouse cells

Cells from a normal mouse mammary epithelial cell line, NMuMG (ATCC), were stably transfected with Green Fluorescent Protein (NMuMG-GFP), as previously described²². Cells from a cancer mouse epithelial cell line (as previously described, cells isolated from a



mammary tumor that spontaneously arose in a MMTV-neu transgenic female mouse²³) were stably transfected with Red Fluorescent Protein (MMTV-neu-RFP)²². NMuMG-GFP cells were cultured in Dulbecco's Modified Eagle's Medium (DMEM, Invitrogen) supplemented with 10% fetal bovine serum (FBS, Gibco), and Mammary Epithelial Cell Growth Medium (MEGM) single quotes (Lonza) while MMTV-neu-RFP cells were cultured in DMEM (Invitrogen) supplemented with 10% FBS (Gibco), 10,000 U penicillin, and 10 mg streptomycin/mL (Sigma-Aldrich). Cells were cultured in a T150 flask (Corning) and maintained in a humidified incubator at 37°C and 5% CO₂. Once cells reached confluence, NMuMG-GFP at passage 4 and MMTV-neu-RFP at passage 5, they were detached using trypsin-EDTA solution (Sigma) and resuspended in growth medium.

Cell culture of human cells

Cells from a mammary epithelial cell line from benign breast tissue, MCF-10A (ATCC), were stably transfected with Green Fluorescent Protein (MCF-10A-GFP)²². Cells from a human breast cancer cell line, MCF-7, (ATCC) were stably transfected with Red Fluorescent Protein (MCF-7-RFP). To perform the lentiviral transfection of the MCF-7 cells, MCF-7 cells were seeded in a 96 well plate in normal growth medium and proliferated in an incubator at 37°C. The media was removed and Cignal Lentiviral particle-RFP (Qiagen; Venlo, Netherlands) with SureENTRY transduction reagent (Qiagen; Venlo, Netherlands) in growth media without antibiotics was added. The plate was incubated for 18-20 hrs, after which the media containing the lentiviral particles was removed and normal growth media containing antibiotics was added and the MCF-7 cells were allowed to grow to confluency. Once confluent growth media containing the selective agent, 2 ug/ml puromycin (Fisher; Fair Lawn, NJ) was added. The selection media was replaced every 3-4 days until puromycin resistant positive colonies appeared. The RFP-positive cells were expanded in selection media to obtain RFP

positive cultures.

MCF-10A-GFP cells, passage 5, were cultured in DMEM (Invitrogen) supplemented with 10% FBS (Gibco), 1% fungizone, and MEGM single quotes (Lonza). MCF-7-RFP cells, passage 6, were cultured in DMEM (Invitrogen) supplemented with 10% FBS, 1% fungizone (Gibco), 10,000 U penicillin, and 10 mg streptomycin/mL (Sigma-Aldrich). Cells were cultured in a T-150 flask (Corning) and maintained in a humidified incubator at 37°C and 5% CO₂. Once cells reached confluence, both cell types were removed with trypsin-EDTA solution (Sigma-Aldrich) and resuspended in culture medium to prepare for vertical testing.

Preparation of fibers

Poly-L-lactide (Natureworks) was extruded to obtain fibers with non-circular cross-sectional dimensions of 0.72 mm x 0.55 mm. Wicking fibers were sliced with a razor blade into individual single wicking fibers of 3.5 cm and 10 cm lengths. The 10-cm wicking fibers were used to form the wicking fiber bundles. To form bundles, three fibers were twisted, using a power drill, at 110 rotations per 10-cm fiber length. Each bundle was sliced into 3.5 cm lengths. Single and bundled wicking fibers were cleaned in three changes of ethanol, for 1 hour each, and placed under ultraviolet light for 6 hours. Samples were then soaked in a phosphate-buffered saline (PBS, Invitrogen) solution for 2 hours and air-dried overnight in a sterile hood. A total of eight single fibers and fifteen 3-fiber bundles were prepared.

Testing of vertical wicking with individual fibers

The vertical wicking test of cells, shown in **Fig. 2**, includes a custom-made culture lid for a low-attachment 12-well plate (Corning). The lid contains fitted holes with columns to securely hold the 3.5 cm wicking fibers and wicking fiber bundles in a vertical position. A 50/50 mix of cancer (NMuMG-GFP) and normal (MMTV-neu-RFP) mouse cells were seeded in eight wells of a low attachment 12-well plate, at a density of one million cells per well (5×10^5 MMTV-neu-RFP and 5×10^5 NMuMG-GFP), along with 1 mL of growth medium per well. Eight single wicking



fibers were vertically inserted through the columns, one per well, so only the bottom 3 mm of the fiber contacted the cell solution. The custom 12-well plate set up was placed on a flat top shaker (VWR) at 100 rpm in a humidified incubator at 37°C and 5% CO₂. The vertical displacements of the cancerous and normal mouse mammary cells along the wicking fibers were determined at time points of 0.5 and 24 hours, with time point 0 being fiber placement into the cell solution. Four fibers were assessed after 0.5 hours, the remainder after 24 hours.

The vertical displacements of the cancerous (MCF-7-RFP) and benign (MCF-10A-GFP) human epithelial cells along the bundles were determined at time points of 0.25 hours, 2 hours, 12 hours and 24 hours, with time point 0 being fiber placement into the cell solution. A similar set-up to the single fiber experiment was conducted, with fifteen 3-fiber bundles, each bundle populating a well of a 12-well plate. Twelve of the bundles were designated for image analysis of cell displacement and the remaining three were designated for quantitative analysis. To assess the cell displacement of both cell types, three fiber bundles were transferred to a 6-well plate, one bundle per well, at each timepoint. Qualitative assessments were made and photographs were taken to document the progression of cells along the length of the bundle at each timepoint. The bundles were rinsed twice with phosphate-buffered saline solution, and fixed for 15 min with 4% paraformaldehyde. After the cells on the wicking fiber constructs were fixed, the fibers were transferred to microscope slides and the vertical displacement was evaluated using fluorescent microscopy and imaging software. The entire length of each bundle was imaged, using fluorescent microscopy, beginning with the seeded end of the wicking fiber construct, using 25x total magnification. A fluorescein isothiocyanate (FITC) filter was used to view the vertical movement of normal cells transfected with Green Fluorescent Protein, and a tetramethyl rhodamine iso-thiocyanate (TRITC) filter was used to view the vertical movement of cancer cells transfected with Red Fluorescent Protein. Imaging software (ImageJ, National

Institutes of Health) was used to determine the vertical displacement (μm) of the cells along the fiber. Images were aligned to qualitatively show the total displacement of both normal and cancer cells, with total vertical displacement quantified by the maximum summation of the displacements in the individual images.

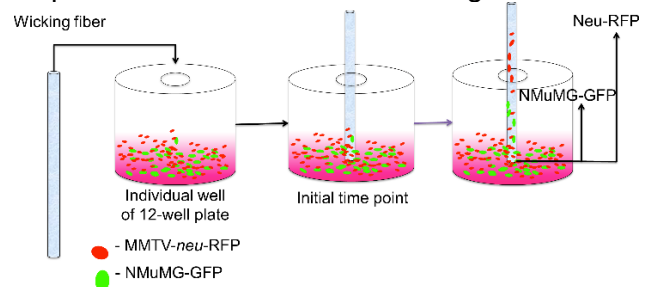


Figure 2. Schematic of vertical wicking test apparatus. The lid of the low-attachment 12-well plate was modified with holes and fitted columns to support the wicking fiber in the vertical position. Cancer and normal cells, tracked with specific fluorescent proteins, were added to each individual well at equivalent cell densities. The wicking fiber or wicking fiber bundle was vertically placed through the column and into a mixed cellular solution so 3 mm of the bottom fiber region was submerged. The fiber was removed at various time points to analyze the vertical cell movement.

Isolation of cancer cells from wicking fiber bundle

After 24 hours, the remaining three vertical wicking fiber bundles were removed from the customized 12-well plate and the fibers were sectioned, with a razor blade, to separate the top and bottom fiber regions. The fiber sections were placed in separate wells of a 24-well plate. The samples were rinsed with PBS twice and untwisted using forceps. The cells were removed by adding 500 μL of tris-ethylenediaminetetraacetic acid (EDTA) solution to the well with the fiber and placing the plate on a flat-top (VWR) shaker at 200 rpm in a 37°C incubator. After 15 min, the cells were resuspended in 500 μL of growth medium and the number of MCF-10A and MCF-7, in both regions of the fibers, was evaluated using a Guava easyCyte™ flow cytometer (Guava Technologies). The number of MCF-10A-GFP



and MCF-7-RFP was determined for each region, following the manufacturer's instructions for InCyte software (Guava Technologies). Positive and negative controls with known cell densities were used to calibrate the machine before measurements of the treatment groups were made.

Determination of cell size

The average cell size of MCF-7-RFP and MCF-10A-GFP cells was measured in cell solution. MCF-7-RFP cells were removed from culture flasks with trypsin-EDTA solution. After incubation with solution for 15 min, 5×10^5 cells were resuspended in 1 mL of growth medium in a 15 mL centrifuge tube. The centrifuge tube was vortexed to maintain the cells in solution. A volume of 100 μ L of cell solution was added to each of three microscope slides. Similarly, three slides of MCF-10A-GFP cells were prepared. The cellular slides were imaged with the fluorescence microscope and measured with imaging software (ImageJ). The measurement function of the software was used to determine the average diameter of each cell line.

Imaging of wicking bundle cross-sections

Wicking fiber bundles, each containing three individual fibers of non-circular cross-sectional dimensions of 0.72 mm x 0.55 mm, were sectioned into 3-cm lengths. Samples were placed vertically in embedding molds for the microtome and infiltrated and embedded with Embed-it™ Low Viscosity Epoxy Resin (Polysciences, Inc.). The wicking fiber samples were embedded and sectioned, following the manufacturer's protocol. Sections, 5 μ m in thickness, were cut with a microtome and transferred to microscope slides. The sections were imaged with a light microscope, and ImageJ imaging software was used to measure and characterize the inter- and intra- fiber spaces.

Statistical analysis

Matched pairs analysis was conducted using JMP statistical software to compare ($p < 0.05$) the vertical displacement of MMTV-neu-RFP (mouse cancer cells) and NMuMG-GFP (normal mouse cells) at 0.5 and 24 hours. A matched pairs analysis was also used to compare

($p < 0.05$) the fraction of MCF-7-RFP cells in top and bottom regions of the fiber bundle. The results showed there were significantly more MCF-7-RFP cells in the top region of the fiber bundles than in the bottom region.

Results

Mouse cancer cell separation using wicking fiber system

We developed a vertical test system (**Fig. 2**) to analyze the vertical movement of different cell mixtures along individual fibers. The vertical displacements of mouse mammary normal cells expressing green fluorescent protein (NMuMG-GFP) and mouse mammary cancer cells expressing red fluorescent protein (MMTV-neu-RFP) were determined at time points of 0.5 and 24 hours using fluorescence microscopy. **Fig. 3** is a composite of fluorescent images, showing the cancer and normal cells along the length of the fiber, aligned to qualitatively show the total displacement of both cell types after 24 hours of contacting cell solution. **Fig. 3A** demonstrates that MMTV-neu-RFP cells, labeled red, have vertically displaced 16.2 mm along the wicking fiber after 24 hours. **Fig. 3B** shows NMuMG-GFP cells, labeled green, vertically moved 3.0 mm, significantly less than the MMTV-neu-RFP cells, on the same wicking fiber. Images also depict higher cell densities of MMTV-neu-RFP cells along the fiber. Images qualitatively show a vertical separation of MMTV-neu-RFP and NMuMG-GFP cells, indicating different cell types move differently along the wicking fibers. Imaging software was used to quantify the vertical displacement (μ m) of the cells along the length of the fiber. The total vertical displacement was found by assessing each individual image. The vertical displacement of the cancer cells, MMTV-neu-RFP, along the wicking fiber was significantly ($p < 0.05$) greater than that of the normal cells (NMuMG-GFP) at the 24-hour time point (**Fig. 3C**). No significant difference was shown after 0.5-hour time point.

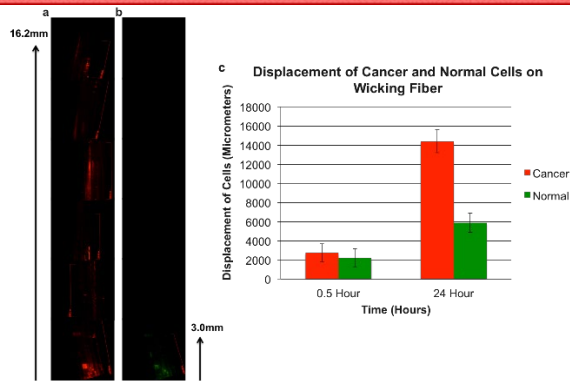


Figure 3. Visualization and quantification of the vertical displacement of cancer and normal cells. The 3.0 mm arrow indicates the portion of fiber in solution. Left image A depicts compiled fluorescent images of the vertical displacement of MMTV-neu-RFP, cancer cells, along the length of the fiber after 24 hours. Image B shows NMuMG-GFP, normal cells, progressed significantly less than the cancer cells. Graph shows quantitative analysis of the vertical displacement of cancer cells (2757 ± 928.9 (SD), $n=4$) and mouse normal cells (2219 ± 940.6 (SD), $n=4$) after various time points. After 24 hours there was significantly greater vertical displacement of MMTV-neu-RFP (14380 ± 1192 (SD), $n=4$) than displacement of NMuMG-GFP (6220 ± 994.2 (SD), $n=4$). $p < 0.05$, indicated by (*) in graph.

Human cancer cell separation and isolation using wicking fiber system

To enhance the effects of individual wicking fibers on cancer cell separation, we developed a wicking fiber bundle that demonstrated improved wicking properties, i.e. the overall wicking rate and volume of liquid transported were enhanced over that of single fibers. The wicking fiber bundle was used to separate and isolate malignant human breast epithelial cells expressing red fluorescent protein (MCF-7-RFP) from benign human breast epithelial cells expressing green fluorescent protein (MCF-10A-GFP). Fluorescent images of the bundles were used to evaluate the vertical displacement and separation of MCF-7-RFP and MCF-10A-GFP after 0.25, 2, 12, and 24 hours. Images show that, after 0.25 hours and 2 hours, MCF-7-RFP cells progressed along the entire fiber but

in low numbers. After 12 and 24-hour time points, much higher numbers of MCF-7-RFP traveled to the top region of the fiber. Images indicate after 0.25 hours, few benign epithelial cells progressed along the fiber bundles. To quantify the number of cancerous and benign cells along the fiber bundles after 24 hours, cells were removed from top and bottom regions of the bundles (**Fig. 4**). The number of MCF-7-RFP and MCF-10A-GFP cells was determined using flow cytometry (Guava Technologies) with InCyte software (Guava Technologies). **Fig. 4** illustrates the percentage of each cell type in top and bottom regions; there is a significant difference ($p < 0.05$) between the percentage of MCF-7-RFP and the percentage of MCF-10A-GFP in the top region of the fiber bundles. These results suggest that the wicking fiber bundle separates cancerous cells from a mixture; as the graph indicates, 82% of cells isolated from the top fiber bundle regions are cancerous.

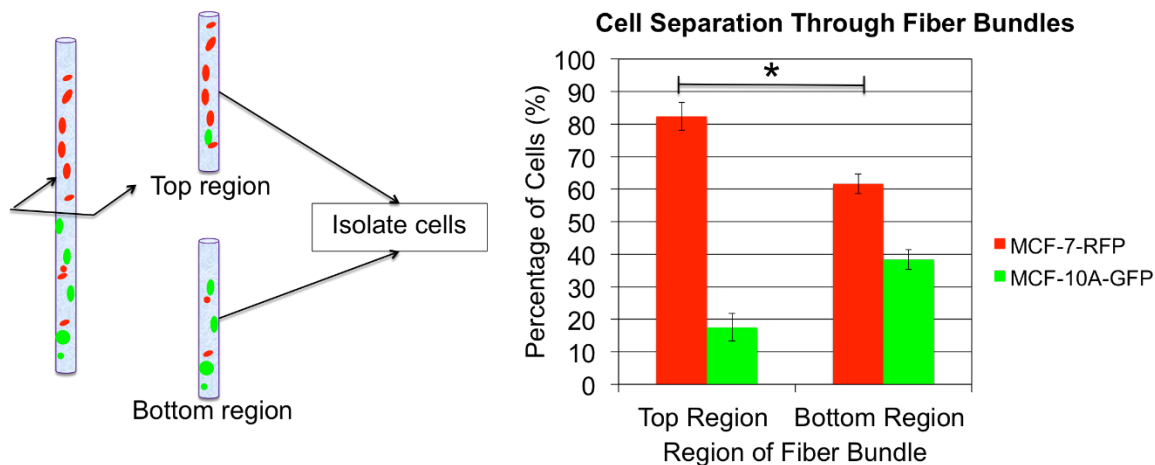


Figure 4. Schematic of the fiber regions and data depicting percentage of each cell type in fiber regions. Left image illustrates axial slicing of fiber bundle to extract top and bottom region cells. Graph exhibits quantitative analysis of top and bottom regions of the fiber bundles after 24 hours, demonstrating significantly higher concentration of MCF-7-RFP cells in the top region of the fiber bundle (82.4 ± 4.3 (SD), $n=3$ bundles) than the bottom region of the fiber bundle (61.6 ± 3.04 (SD), $n=3$ bundles) The graph indicates a significantly lower concentration of MCF-10A-GFP cells in top region (17.6 ± 4.3 (SD), $n=3$ bundles) than bottom region (38.4 ± 3.04 (SD), $n=3$ bundles) (* indicates significant difference, $p < 0.05$).

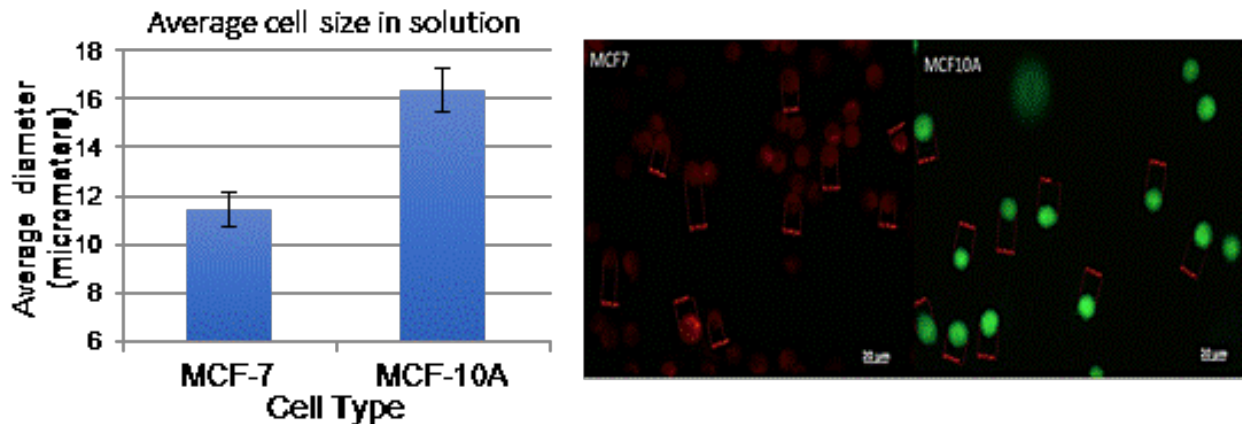


Figure 5. Fluorescent images of MCF-7 and MCF-10A cells in solution. Imaging software was used to measure diameters (indicated in red) of both cell types in solution, see images above, each bar is the average of three 100 μ L samples. Left image shows smaller diameter MCF-7 cells and right image reveals larger diameter MCF-10A cells. The graph shows the average diameters of the cancerous and benign cell types. The cancerous cells, MCF-7s, are significantly smaller ($p < 0.05$) than the benign cells, MCF-10As.

Determination of cell size and wicking bundle cross-sections

Fluorescent imaging and imaging software was used to determine the average cell size of cancer and normal cells in solution; MCF-7-RFP

cells are significantly smaller, by approximately 5 μ m, than MCF-10A-GFP (**Fig. 5**). To understand the interaction that cell size may have on migration, cross-sectional images of the wicking fiber bundle were taken. These images depict channel and interfiber space sizes (**Fig. 6**).

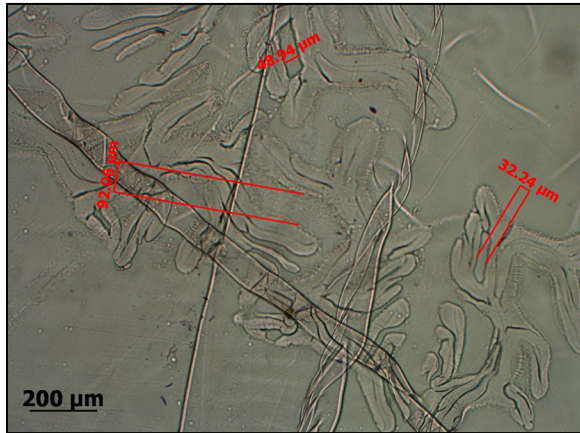


Figure 6. Axial cross-section of a representative wicking fiber bundle illustrates channels and inter-fiber spaces up to 95 μ m. The inter- and intra- fiber spaces affect capillary pressure and ability for fluid and cells to penetrate the fiber and vertically move through the fiber. Cell size and deformability will influence the ability of the cells to penetrate and travel through the intra- or inter- fiber spaces.

Discussion

Our wicking fiber device has potential to separate, isolate, and identify cancerous breast epithelial cells from a mixture containing benign breast epithelial cells. The separation is due to the physical and functional properties of the cells, wicking characteristics of the fiber bundle, and the cell-fiber interaction. Physical properties that may play a role include cell size, deformability, surface friction or charge, and expression of cell adhesion molecules. The size and shape of the cells may play a role in the ability of cells to penetrate the smaller channels created from the bundling of the fibers. Fiber bundle architecture will affect the wicking rate and vertical displacement of different cell types. The size of the individual fibers, the tension of the bundle, the hydrophobicity, and the inter-fiber space will play a role in the wicking of liquid as well as cell-interaction. Further studies are necessary to reveal which characteristics are most influential on wicking and the relevant underlying mechanistic principles.

Other cellular properties influencing vertical movement include cell membrane impedance, expression of adhesion molecules, and cell stiffness. Membrane impedance, cell dielectric properties or cell electric properties vary between cell types^{24,25}. Electrical properties of the cell will influence the cell-interaction with the fiber and the resultant vertical movement. Cells with greater impedance or surface charge may have more interactions with the fiber, thus hindering the vertical cell movement. Abdolhab and coworkers evaluated the cellular impedance for cancer cells of varying aggressiveness and demonstrated that a more aggressive cancer cell type (MDA-MD231) has significantly lower impedance than a less aggressive cancer cell (MCF-7). Additionally they found a correlation between metastatic progression and membrane impedance reduction. Cell-fiber interaction and overall cell displacement will be affected by different membrane impedances.

Expression of cell adhesion molecules can play a role in the cell-fiber interaction and ability of a cell to move through a confined space. Metastatic cells are known to lose endothelial adhesion molecules and transition into more motile mesenchymal phenotypes¹². Cancerous cells with fewer adhesion molecules may have less surface friction and altered shapes that have less interaction with the fibers, allowing the cells to wick greater distances.

Cell deformability will influence the ability for cells to deform, penetrate, and wick vertically through the twisted channels. Researchers have generally shown that cancer cells have a significantly lower Young's modulus compared to that of normal cells^{26,27,28}. Researchers have found that cancer cells of increased metastatic potential have higher deformability^{29,30}. This point suggests that MCF-7 cells are much softer and deform more easily than normal cells, allowing the cancer cells to migrate more readily. Microfluidic devices have been employed to distinguish cancer and normal cells, based on cellular deformability, by analyzing the ability of cells to squeeze and pass through confined constrictions^{28,31,32}. Indeed, Li and coworkers found the apparent



Young's modulus of MCF-10A, non-malignant breast epithelial cells, to be significantly higher than that of MCF-7³³. The softer cytoskeleton and deformability of the MCF-7 cells may play a role in their ability to squeeze through channels and wick upward through the confined spaces.

We demonstrated the wicking fiber approach can separate normal mouse mammary epithelial cells (MMTV-neu) from mouse breast cancer cells and (NMuMG). We showed the wicking fiber bundle rapidly separates human cancerous breast cells from human benign breast cells. Fluorescent images indicate separation of cells after 15 min of fiber bundle contact with cellular liquid. After 24 hours, large quantities of cells penetrated the fibers, and cancerous breast cells were efficiently isolated from the top region of the fiber. Properties of the fiber and cells will influence the cell-fiber interaction and resultant separation of the cells. The architecture, material properties, and surface properties of the fiber bundle will influence the separation of cells and their wicking profiles. Relevant cell properties, including cell surface charge, cell stiffness, cell size, and cell surface adhesion molecules, will vary between cancerous cells of different metastatic potential and play a role in cell-fiber interaction and the ability of cells to wick through the channels.

We have developed a simple, inexpensive approach to separate cancer cells from benign cells; the approach could be applied to separating cancerous cells of varying metastatic potential. Current diagnostic methods are time-consuming, expensive, and lack information. The current methods require external laboratories with complex systems and trained research personnel to perform multiple tests to confirm results. Common reliance on biomarkers may only capture a small cellular subpopulation of a heterogeneous tumor and does not provide information about the metastatic potential of the cancer cells. The rigid design of microfluidic devices that separate cancer cells requires the use of an external pump and antigen labels, which limits the populations of cancer cells targeted. These technologies are only capable of analyzing small

amounts of sample and provide limited information about the metastatic potential of heterogeneous populations within the tumor. Our simple and rapid approach allows the analysis of large volumes of liquid biopsy and requires no external pump. Our results demonstrate this device can separate cancerous breast epithelial cells from benign breast epithelial cells based on their wicking capabilities. The flexible design of the fiber bundle allows identification and separation of subpopulations of varying metastatic potential within a tumor. The wicking fiber diagnostic may provide a rapid approach to identify cancer cells from a liquid biopsy that can easily be translated into a method for on-site clinic testing.

Acknowledgments

Funding for the work was provided, in part, by the Avon Foundation for Women Grant 02-2013-076 and the Clemson University Hunter Endowment.



References

1. Crowley, E., F. Di Nicolantonio, F. Loupakis, and A. Bardelli. Liquid biopsy: monitoring cancer-genetics in the blood. *Nat. Rev. Clin. Oncol.* 10:472–484, 2013.
2. Hanahan, D., and R. Weinberg. Hallmarks of cancer: the next generation. *Cell* 144:646–674, 2011.
3. Magee, J. A., E. Piskounova, and S. J. Morrison. Cancer stem cells: impact, heterogeneity, and uncertainty. *Cancer Cell* 21:283–296, 2012.
4. Almendro, V., A. Marusyk, and K. Polyak. Cellular heterogeneity and molecular evolution in cancer. *Annu. Rev. Pathol.* 8:277–302, 2013.
5. Charafe-Jauffret, E., C. Ginestier, F. Iovino, J. Wicinski, N. Cervera, P. Finetti, M.-H. Hur, M. E. Diebel, F. Monville, J. Dutcher, M. Brown, P. Viens, L. Xerri, F. Bertucci, G. Stassi, G. Dontu, D. Birnbaum, and M. S. Wicha. Breast cancer cell lines contain functional cancer stem cells with metastatic capacity and a distinct molecular signature. *Cancer Res.* 69:1302–1313, 2009.
6. Cho, R. W., and M. F. Clarke. Recent advances in cancer stem cells. *Curr. Opin. Genet. Dev.* 18:48–53, 2008.
7. Li, P., Z. S. Stratton, M. Dao, J. Ritz, and T. J. Huang. Probing circulating tumor cells in microfluidics. *Lab Chip* 13:602–609, 2013.
8. Nagrath, S., L. V. Sequist, S. Maheswaran, D. W. Bell, P. Ryan, U. J. Balis, R. G. Tompkins, and D. A. Haber. Isolation of rare circulating tumour cells in cancer patients by microchip technology. *Nature* 450:1235–1239, 2007.
9. Yoon, H. J., T. H. Kim, Z. Zhang, E. Azizi, T. M. Pham, C. Paoletti, J. Lin, N. Ramnath, M. S. Wicha, D. F. Hayes, D. M. Simeone, and S. Nagrath. Sensitive capture of circulating tumour cells by functionalized graphene oxide nanosheets. *Nat. Nanotechnol.* 8:735–742, 2013.
10. Harris, J. L., M. Stocum, L. Roberts, C. Jiang, J. Lin, and K. Spratt. Quest for the ideal cancer biomarker: an update on progress in capture and characterization of circulating tumor cells. *Drug Dev. Res.* 74:138–147, 2013.
11. van de Stolpe, A., K. Pantel, S. Sleijfer, L. W. Terstappen, and J. M. J. Den Toonder. Circulating tumor cell isolation and diagnostics: toward routine clinical use. *Cancer Res.* 71:5955–5960, 2011.14.
12. Wirtz, D., K. Konstantopoulos, and P. Searson. The physics of cancer: the role of physical interactions and mechanical forces in metastasis. *Nat. Rev. Cancer* 11:512–522, 2012.
13. Yu, M., A. Bardia, B. S. Wittner, S. L. Stott, M. E. Smas, D. T. Ting, S. J. Isakoff, J. C. Ciciliano, M. N. Wells, A. M. Shah, K. F. Concannon, M. C. Donaldson, L. V. Sequist, E. Brachtel, D. Sgroi, J. Baselga, S. Ramaswamy, M. Toner, D. A. Haber, and S. Maheswaran. Circulating breast tumor cells exhibit dynamic changes in epithelial and mesenchymal composition. *Science* 339:580–584, 2013.
14. Marie-Egyptienne, D. T., I. Lohse, and R. P. Hill. Cancer stem cells, the epithelial to mesenchymal transition (EMT) and radioresistance: Potential role of hypoxia. *Cancer Lett.* 341:63–72, 2013.
15. Hung, L. Y., Y. H. Chuang, H. T. Kuo, C. H. Wang, K. F. Hsu, C. Y. Chou, and G. B. Lee. An integrated microfluidic platform for rapid tumor cell isolation, counting and molecular diagnosis. *Biomed. Microdevices* 15:339–352, 2013.
16. Hilbert, K. J., and R. K. Marcus. Separation of water-soluble polymers using capillary-channeled polymer fiber stationary phases. *J. Sep. Sci.* 33:3571–3577, 2010.
17. Nelson, D. K., and R. K. Marcus. A novel stationary phase: capillary-channeled polymer (C-CP) fibers for HPLC separations of proteins. *J. Chromatogr. Sci.* 41:475–479, 2003.
18. Pittman, J. J., V. Klep, I. Luzinov, and R. K. Marcus. Extraction of metals from aqueous systems employing capillary-channeled polymer (C-CP) fibers modified with poly(acrylic acid) (PAA). *Anal. Methods* 2:461–469, 2010.
19. Burg, K. J. L., and D. Brunson. A novel use for capillary channel fibers: enhanced engineered tissue systems. *IEEE EMBS Annu. Int. Conf.* 2358–2361, 2006.
20. Marcus, R. K., W. C. Davis, B. C. Knippel, L. LaMotte, T. A. Hill, D. Perahia, and J. D. Jenkins. Capillary-channeled polymer fibers as stationary phases in liquid



- chromatography separations. *J. Chromatogr. A* 986:17–31, 2003.
21. Stanelle, R. D., L. C. Sander, and R. K. Marcus. Hydrodynamic flow in capillary-channel fiber columns for liquid chromatography. *J Chromatogr A* 1100:68–75, 2005.
22. Park J. P., W. M. Blanding, J. A. Feltracco, and B. W. Booth. Validation of an in vitro model of erbB2+ cancer cell redirection. *In Vitro Cell. Dev. Biol.-An.* 51:776-786, 2015.
23. Xu C., J. F. Langenheim, W. Y. Chen. Stromal–epithelial interactions modulate cross-talk between prolactin receptor and HER2/Neu in breast cancer. *Breast Cancer Res. Treatment.* 134:157-169, 2012.
24. Becker, F. F., X. B. Wang, Y. Huang, R. Pethig, J. Vykoukal, and P. R. Gascoyne. Separation of human breast cancer cells from blood by differential dielectric affinity. *PNAS* 92:860–864, 1995.
25. Zou, Y., and Z. Guo. A review of electrical impedance techniques for breast cancer detection. *Med. Eng. Phys.* 25:79–90, 2003.
26. Lekka, M., D. Gil, K. Pogoda, J. Dulińska-Litewka, R. Jach, J. Gostek, O. Klymenko, S. Prauzner-Bechcicki, Z. Stachura, J. Wiltowska-Zuber, K. Okoń, and P. Laidler. Cancer cell detection in tissue sections using AFM. *Arch. Biochem. Biophys.* 518:151–156, 2012.
27. Suresh, S. Biomechanics and biophysics of cancer cells. *Acta Biomater.* 3:413–438, 2010.
28. Zhang, W., K. Kai, D. S. Choi, T. Iwamoto, Y. H. Nguyen, H. Wong, M. D. Landis, N. T. Ueno, J. Chang, and L. Qin. Microfluidics separation reveals the stem-cell-like deformability of tumor-initiating cells. *PNAS* 109:18707–18712, 2012.
29. Swaminathan, V., K. Mythreye, E. O'Brien, A. Berchuck, G. Blobe, and R. Superfine. Mechanical stiffness grades metastatic potential in patient tumor cells and in cancer cell lines. *Cancer Res.* 71:5075–5080, 2011.
30. Xu, W., R. Mezencev, B. Kim, L. Wang, J. McDonald, and T. Sulchek. Cell stiffness is a biomarker of the metastatic potential of ovarian cancer cells. *PLoS One* 7:e46609, 2012.
31. Byun, S., S. Son, D. Amodei, N. Cermak, J. Shaw, J. Ho, and V. C. Hecht. Characterizing deformability and surface friction of cancer cells. *PNAS* 110:7580–7585, 2013.
32. Shim, S., M. G. Kim, K. Jo, Y. S. Kang, B. Lee, S. Yang, S.-M. Shin, and J.-H. Lee. Dynamic characterization of human breast cancer cells using a piezoresistive microcantilever. *J. Biomech. Eng.* 132:104501, 2010.
33. Li, Q. S., G. Y. H. Lee, C. N. Ong, and C. T. Lim. AFM indentation study of breast cancer cells. *Biochem. Biophys. Res. Commun.* 374:609–613, 2008.